electronic reprint

FOUNDATIONS
ADVANCES

ISSN: 2053-2733
journals.iucr.org/a

Computer simulations of X-ray spherical wave dynamical diffraction in one and two crystals in the Laue case

V. G. Kohn and I. A. Smirnova

Acta Cryst. (2018). A**74**, 699–704

IUCr Journals
CRYSTALLOGRAPHY JOURNALS ONLINE

Copyright © International Union of Crystallography

Author(s) of this paper may load this reprint on their own web site or institutional repository provided that this cover page is retained. Republication of this article or its storage in electronic databases other than as specified above is not permitted without prior permission in writing from the IUCr.

For further information see http://journals.iucr.org/services/authorrights.html

Acta Cryst A FOUNDATIONS ADVANCES

ISSN 2053-2733

Computer simulations of X-ray spherical wave dynamical diffraction in one and two crystals in the Laue case

V. G. Kohn[a]* and I. A. Smirnova[b]

[a]National Research Centre 'Kurchatov Institute', 123182 Moscow, Russia, and [b]Institute of Solid State Physics RAS, 142432 Chernogolovka, Moscow district, Russia. *Correspondence e-mail: kohnvict@yandex.ru

Received 6 July 2018
Accepted 5 September 2018

Edited by L. D. Marks, Northwestern University, USA

Keywords: X-ray diffraction; diffraction focusing; compound refractive lens; synchrotron radiation; XFEL energy spectrometer.

This article reports computer simulations of X-ray spherical wave dynamical diffraction in one and two single crystals in the Laue case. An X-ray compound refractive lens (CRL) as a secondary radiation source of spherical waves was considered for the first time and in contrast to previous simulations with the assumption of the use of a slit. The main properties of the CRL as a secondary source are discussed and two focusing phenomena are analysed. The first one is the diffraction focusing effect for one single crystal in the reflected beam and in the case of a large source-to-detector distance. The second one is the same but for two single crystals and for the twice-reflected beam in the case of a short distance between the source and detector. The first effect is well pronounced in the case of strong absorption. However, it may also be used as an element of an energy spectrometer in the medium and even weak absorption case. The second effect will appear in the case of weak absorption. It is shown that it is not effective to use it in an energy spectrometer. In the case of weak absorption the transverse size of the diffraction focused beam will oscillate together with the reflected beam integral intensity. The oscillation period is close to the extinction length.

1. Introduction

The X-ray dynamical diffraction theory for monochromatic plane waves in ideal crystals was developed in the first half of the 20th century by Ewald and Laue (Pinsker, 1978; Authier, 2005). However, for a long time it was impossible to verify the theory because of the absence of thick, perfect crystals and also because of a lack of ways to generate monochromatic plane waves. The first successful experiment was performed in 1959 using an experimental setup with a narrow slit in front of a crystal in the Laue case where both transmitted and reflected beams exit the crystal through the surface that is opposite to the entrance surface (Kato & Lang, 1959). To describe the observed *Pendellösung* fringes Kato (1961) developed the theory for this experimental setup. He named it the theory of X-ray spherical wave diffraction.

Actually, Kato's theory was developed for a point source at the entrance surface of a crystal. The task was analytically solved through Bessel functions. Later on it was shown that this solution is the crystal propagator which allows calculation for the general case of an arbitrary incident wave by means of a convolution (Afanas'ev & Kohn, 1971). Such a solution matches Takagi's (1962) equations solution. Several years later Afanasev & Kon (1977*a*,*b*) showed that the distance between a point source and a detector may significantly change the results in this experimental setup.

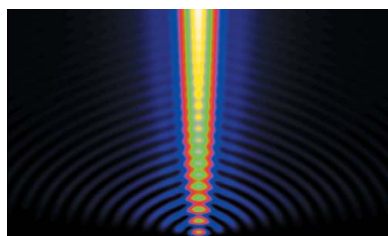

© 2018 International Union of Crystallography

electronic reprint

Moreover, the diffraction focusing effect was discovered while half of the radiation intensity becomes localized at a detector in a small transverse region, if $t = t_0$ where t is the crystal thickness, $t_0 = C_0 L$ is the characteristic thickness that is proportional to the distance L between the source and detector, and C_0 is a very small dimensionless coefficient. The feature of this focusing effect is that just a spherical wave, but not a plane one, may be focused. It is similar to a light focusing (Pendry, 2000) lens made with metamaterial of negative refraction index. In the case of X-ray radiation negative refraction occurs for half of the wavefield that is absorbed weakly in a narrow angular region near the Bragg angle.

X-ray spherical wave dynamical diffraction in one crystal for any source-to-detector distance was investigated both theoretically and experimentally in a series of works (Aristov *et al.*, 1978, 1980, 1982; Kohn, 1979; Kohn *et al.*, 2000, 2013; Koz'mik & Mihailiuk, 1978; Shulakov & Smirnova, 2001). Recently, a new type of energy spectrometer for X-ray free-electron lasers (XFELs) was proposed using diffraction focusing (Kohn *et al.*, 2013).

Nevertheless, until now the properties of diffraction focusing by one crystal have not been studied completely. In early works an X-ray tube as a source and a narrow slit in front of the crystal were assumed. Today the third-generation synchrotron radiation (SR) sources allow researchers to obtain much more detailed information about X-ray beam transformation by the crystal. The source-to-detector distance is fixed and very large on SR beamlines. Therefore it is necessary to use a secondary source which can be created by an X-ray compound refractive lens (CRL) (Snigirev *et al.*, 1996, 2009; Lengeler *et al.*, 1999).

In this work we present results of accurate computer simulations in the case where a CRL is used as a secondary source of small transverse size. We show that using a CRL in an experiment allows one to study features of X-ray spherical wave diffraction more accurately than by using a slit.

Another diffraction focusing effect was discovered theoretically in the case of two X-ray spherical wave reflections in a system of two crystals of the same thickness $t_1 = t_2$ that are located at a small source-to-detector distance (Indenbom *et al.*, 1974*a*,*b*). This effect was immediately used in the experiment as a kind of energy spectrometer for X-ray radiation (Suvorov & Polovinkina, 1974; Indenbom & Suvorov, 1976) without analysing how the source-to-detector distance varies the size of a beam at the focus.

This question was analysed several years later (Aristov, Snigirev *et al.*, 1986; Aristov *et al.*, 1986*a*,*b*). It was shown that the distance varies the focusing conditions. For crystals of different thicknesses t_1 and t_2 there are three focusing conditions, *i.e.* (i) $t_1 + t_2 = t_0$, (ii) $t_1 = t_2 - t_0$ and (iii) $t_1 = t_2 + t_0$. The first case is similar to a situation where two crystals work like one crystal and only the part of the radiation having a small absorption index is focused. In the second or third cases different parts of the radiation wavefield with different absorption power are focused. When $t_0 = 0$ both the latter conditions are fulfilled simultaneously and one obtains the narrowest beam at the focus.

In this work we study the focusing effect of two crystals through more detailed computer simulations. We show that zero distance can be realized using a CRL when the detector is placed at focal distance from the CRL and a system of two crystals may be located in-between the CRL and detector. In the case of $t_1 = t_2$ the beam size increases rapidly with distance.

2. Experimental setup and method of computer simulations

Let us consider the experimental setup as shown in Fig. 1 in the case of one crystal. In the case of two crystals they are close to one another. However, some small distance is still assumed – to separate in space the transmitted and reflected beams. As may be seen in Fig. 1, the X-ray beam from an SR source located at a large distance z_0 from the CRL is monochromated by a standard Si double-crystal monochromator (M). Then the CRL creates a divergent beam with the origin at a secondary source located at the CRL focus. The CRL aperture is restricted by a slit (S). It prevents X-ray transmission in the area beyond the aperture if the CRL does not completely absorb radiation at the aperture's end.

The beam angular divergence coming from a secondary source (F) is greater than the crystal (C) angular area for dynamical diffraction near the Bragg angle. That is why, using any crystal position, just a part of the CRL aperture is used. But by rotating the crystal one can use any part of the CRL aperture. Such a rocking curve allows one to investigate the CRL aperture quality. As has been shown by Kohn *et al.* (2013), the diffraction focusing effect may be used to measure the X-ray energy spectrum if the crystal is located at the front of the detector.

On the other hand, to obtain a diffraction pattern for monochromatic radiation it is necessary to use a scheme where the crystal is located at equal distances from both the secondary source and detector. Such a location satisfies the condition of polychromatic focusing when pictures for various monochromatic harmonics are located at the same place in the detector.

In the case of monochromatic radiation the picture is independent of the crystal position. It is convenient to assume for computer simulations that the detector is located just

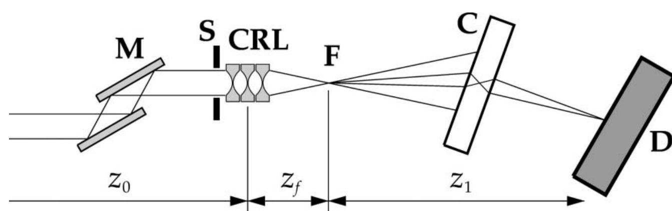

Figure 1
Experimental setup used in computer simulations. Here M is a monochromator, S is a slit, CRL is a compound refractive lens, F is a point of the beam focus (secondary source), C is a crystal, D is a detector.

electronic reprint

behind the crystal. Then, in the case of one crystal, the electric field of the X-ray reflected beam at the detector may be calculated as follows:

$$E(x) = \int \mathrm{d}x_1 P_{\mathrm{C}}(x - x_1) \int \mathrm{d}x_2 P(x_1 - x_2, Z_1) T(x_2) \times P(x_2 - x_0, z_0), \quad (1)$$

where z_0 is the distance from a point source of the SR to the CRL, $Z_1 = z_f + z_1$ is the distance from the CRL to the detector (see Fig. 1).

Here

$$P(x, z) = (i\lambda z)^{-1/2} \exp\left(i\pi \frac{x^2}{\lambda z}\right) \quad (2)$$

is the Fresnel propagator as a transverse part of the spherical wave along the x direction in the paraxial approximation,

$$P_{\mathrm{C}}(x) = \int \frac{\mathrm{d}q}{2\pi} \exp(iqx) P_{\mathrm{C}}(q) \quad (3)$$

is the crystal propagator as a Fourier image of the plane-wave amplitude for reflection by the crystal $P_{\mathrm{C}}(q)$, where q describes an angular deviation $\theta = q/K$, $K = 2\pi/\lambda$, from the Bragg angle θ_{B}.

In the symmetrical Laue case we have

$$P_{\mathrm{C}}(q) = \frac{s}{2b}[\exp(-M - iB) - \exp(-M + iB)] \quad (4)$$

where

$$M = \frac{\mu_0 t}{2\cos\theta_{\mathrm{B}}}, \quad B = \frac{bt}{2\cos\theta_{\mathrm{B}}}, \quad b = (a^2 + s^2 f)^{1/2},$$
$$a = (q - q_0)\sin(2\theta_{\mathrm{B}}), \quad s = KC\chi_h, \quad f = \chi_{-h}/\chi_h. \quad (5)$$

Here $\mu_0 = K\chi_0''$ is a linear absorption coefficient, χ_0'' is the χ_0 imaginary part, and then χ_0, χ_h and χ_{-h} are Fourier components of the crystal susceptibility $\chi = \varepsilon - 1$. ε is the dielectric function, t is the crystal plate thickness, $q_0 = K\theta_0$ and θ_0 is an angular shift of the crystal orientation from the position where the Bragg condition is realized for the plane wave along the optical axis, C is the factor of polarization state, namely $C = 1$ for σ polarization and $C = \cos(2\theta_{\mathrm{B}})$ for π polarization. Details of the derivation of this equation are given in the work of Kohn (2002).

An X-ray beam from a SR source is focused by the CRL. The CRL is described by transmission function $T(x)$ in the thin lens approximation. This function may be written as

$$T(x) = \exp\left[-i\pi \frac{x^2}{\lambda F}(1 - i\gamma)\right]\theta(x_a - |x|), \quad (6)$$

where $F = R/(2N\delta)$, $\gamma = \beta/\delta$, $x_a = A/2$, A is the aperture of the CRL which is equal to the size of the slit in front of the CRL, R is the curvature radius at the elemental double-concave lens (chip) surface apex, N is the number of chips. The complex refraction index of the CRL matter is $n = 1 - \delta + i\beta$.

The source size may be taken into account by coordinate x_0. It defines the transverse shift of a point source from the optical axis. The detector measures the X-ray radiation intensity $I(x) = |E(x)|^2$. In the case of two reflections from two crystals we have an equation that is similar to equation (1):

$$E(x) = \int \mathrm{d}x_1 P_{\mathrm{C}}^2(x - x_1) \int \mathrm{d}x_2 P(x_1 - x_2, Z_1) T(x_2) \times P(x_2 - x_0, z_0), \quad (7)$$

where function $P_{\mathrm{C}}(x)$ is replaced by function $P_{\mathrm{C}}^2(x)$.

Computer simulations are performed with a program based on our own language ACL. The ACL interpreter is a Java program – it is free to download together with a programming language tutorial (Kohn, 2017). These simulations reveal that for crystal diffraction a calculation considering the secondary source at the focus of the CRL is sufficient. This approximation may be verified analytically. We use a property of the Fresnel propagator that convolution of two propagators with distances z_f and z_1 is equal to a propagator with distance Z_1.

Therefore we can replace equation (1) by the following formulae:

$$E(x) = \int \mathrm{d}x_1 P_{\mathrm{C}}(x - x_1) \int \mathrm{d}x_2 P(x_1 - x_2, z_1) B(x_2, x_0), \quad (8)$$

$$B(x, x_0) = \int \mathrm{d}x_1 P(x - x_1, z_f) T(x_1) P(x_1 - x_0, z_0). \quad (9)$$

Function $B(x, x_0)$ describes the radiation field at the CRL focus. Substituting equations (2) and (6) we obtain

$$B(x, x_0) = \frac{A(x, x_0)}{i\lambda(z_f z_0)^{1/2}} \int \mathrm{d}x_1 \exp\left[-i2\pi \frac{(x - x_0')}{\lambda z_f} x_1 - \frac{\pi\gamma}{\lambda F} x_1^2\right], \quad (10)$$

where

$$A(x, x_0) = \exp\left[-i\pi\left(\frac{x^2}{\lambda z_f} + \frac{x_0^2}{\lambda z_0}\right)\right], \quad x_0' = -x_0 \frac{z_f}{z_0}. \quad (11)$$

Here we use the relation $1/z_f = 1/F - 1/z_0$.

The integral (9) can be written as an analytical expression,

$$B(x, x_0) = \frac{A(x, x_0)}{iC_2} G(x - x_0', \sigma) \quad (12)$$

where

$$C_2 = \left(\frac{C_1}{1 - C_1}\right)^{1/2}, \quad C_1 = 1 - \frac{F}{z_0}, \quad \sigma = \frac{1}{C_1}\left(\frac{\lambda F\gamma}{2\pi}\right)^{1/2},$$
$$G(x, \sigma) = \frac{1}{\sigma(2\pi)^{1/2}} \exp\left(-\frac{x^2}{2\sigma^2}\right). \quad (13)$$

From equation (12), the amplitude of the function which describes the transverse part of the focused radiation field is proportional to a Gaussian with an FWHM (full width at half-maximum) $w = 2.355\sigma$.

The Gaussian maximum is shifted by a distance x_0' if the point source is shifted by a distance x_0. Let M be a constant phase factor which does not affect the intensity. Then we can write

$$B(x, x_0) = B(x - x_0', 0) M \exp\left(i\pi \frac{2xx_0'}{\lambda z_f}\right). \quad (14)$$

Equation (14) shows that the radiation field not only becomes shifted, but also acquires an additional phase factor. However, this factor is close to unity because $z_f \ll z_0$ under standard conditions. As a result $|x_0'| \ll |x_0|$, $x \simeq x_0$ and $|xx_0'| \ll \lambda z_f$.

electronic reprint

We note that numerical results presented in this work were obtained using equations (1) and (7) for the point source at the optical axis. The reason is that the source size weakly affects the diffraction pattern because the diffraction focusing effect is weak. We used a standard fast Fourier transformation (FFT) procedure to carry out convolution calculation on the set of $N = 65536 = 2^{16}$ points within a segment of X = 8192 µm, *i.e.* with a step $d = X/N = 0.125$ µm, for high energy or half as much for low energy.

The function $E_0(x) = T(x)P(x, z_0)$ was calculated on this set of points in real space. Then the FFT procedure allowed calculation of $E_0(q)$ on the same set of points but in reciprocal space with a step $\Delta = 2\pi/X$ and the same number of points. Finally, the product $E_0(q)P(q, Z_1)P_C(q)$ was calculated and its result $E(x)$ was acquired by means of the inverse FFT procedure with respect to the initial set of points. Intensity within a useful segment was acquired by means of an interpolation procedure.

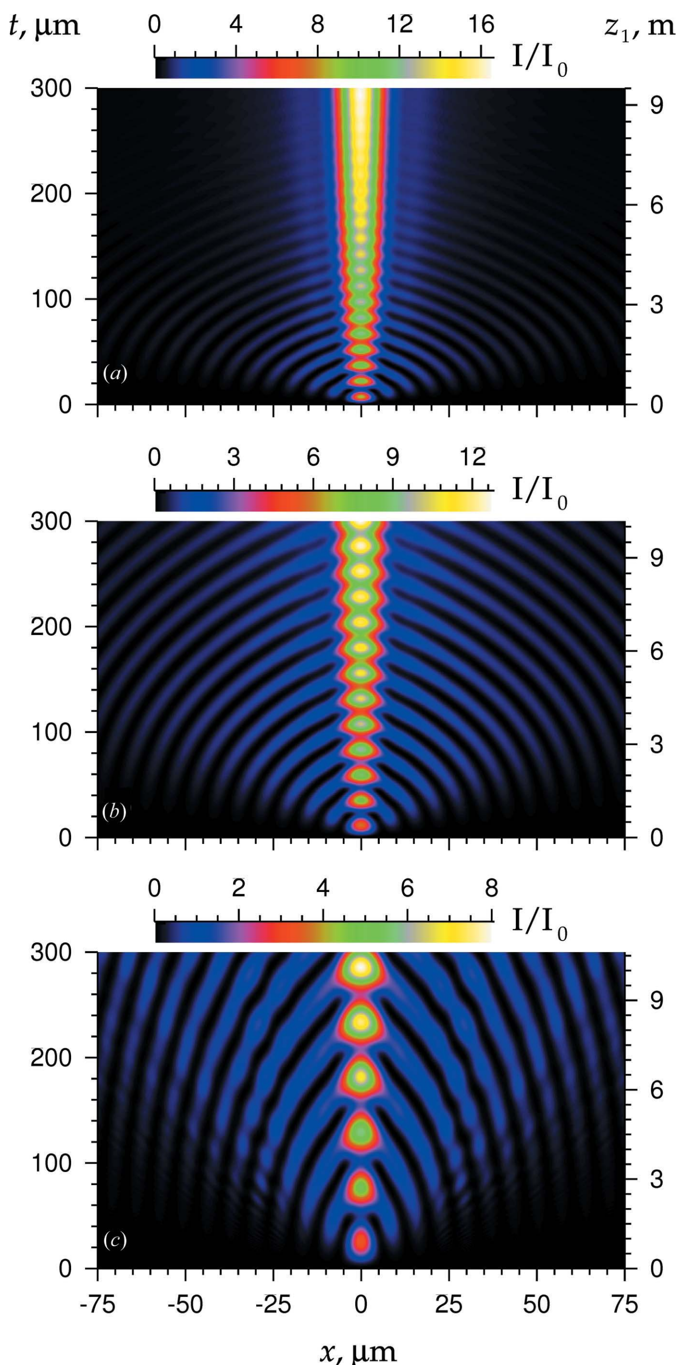

Figure 2
Focused beam transverse intensity distribution as a function of crystal thickness t. Energy of X-ray photons E = 8 keV (a), 12 keV (b) and 25 keV (c). The right-hand axis shows the focusing distance $z_1 = C_0^{-1}t$.

3. Diffraction focusing of an X-ray spherical wave by one single crystal

As was first shown by Afanasev & Kon (1977*a*,*b*) the diffraction focusing effect reveals itself in pure form only under the condition of strong absorption when the strongly absorbing radiation part cannot exit the crystal. However, it is of interest to understand what would happen if this condition were not satisfied. As was pointed out above, diffraction focusing should occur if the crystal thickness $t = t_0$, where $t_0 = C_0L$, $C_0 = 2|\chi_h|\cos\theta_B \sin^{-2}(2\theta_B)$ and $L = z_1$ in our case according to Fig. 1.

Fig. 2 shows the results of the calculation of intensity distribution at the detector (x axis) for various values of crystal thickness t under the condition $t = t_0$. It means that the distance z_1 depends on any value of thickness t according to $z_1 = C_0^{-1}t$. These values of t are placed at the left vertical axis and corresponding values of z_1 at the right vertical one. Three values of photon energy were considered, E = 8 keV (Fig. 2*a*), 12 keV (Fig. 2*b*) and 25 keV (Fig. 2*c*).

The secondary radiation sources were made of planar silicon CRLs that are composed of parabolic shape bi-concave elements (chips) having a curvature radius of 6.25 µm at the apex. These CRLs had six, 14 and 58 chips for energy of 8, 12 and 25 keV, respectively. The focal lengths were approximately the same but more precisely were equal to 6.78, 6.58 and 6.96 cm, respectively.

Fig. 2(*a*) presents the results in the case of soft X-rays with an energy of 8 keV. Within the interval of crystal thickness 200–300 µm the absorption parameter $P = \mu t/\cos\theta_B$ is equal to values within the interval 3.1–4.7, *i.e.* the Borrmann effect is realized but not strongly. Here μ is a linear absorption coef-

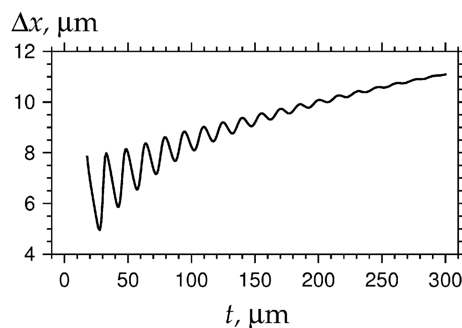

Figure 3
Variation of the focused beam width (FWHM) Δx in the case of one crystal with crystal thickness t for energy E = 8 keV.

electronic reprint

ficient. Therefore the highly absorbing radiation part is decreased to zero but the slightly absorbing one stays on a narrow incidence angle range near the Bragg angle, and the greater the crystal thickness the smaller the size of this range.

Obviously, the greater the angular range of the output beam the smaller is the beam transverse size at the focus. The angular range decreases with crystal thickness. Fig. 3 shows how the beam FWHM Δx depends on crystal thickness in the case of E = 8 keV. It follows from Figs. 2(*a*) and 3 that the net intensity peak (that is free from side oscillations) arises just for thicknesses that are larger than 250 µm and its FWHM is equal to 10 µm.

In the hard radiation case absorption is weak, *e.g.* for E = 25 keV absorption parameter P varies between the values 0.10 and 0.15 at the same thickness interval 200–300 µm. Therefore both strong and weak absorbed radiation fields exit the crystal and they interfere. As a result of this interference in the incident plane-wave case, both the transmitted wave and the reflected one will oscillate with a period that is equal to the extinction length but total intensity remains the same.

A spherical incident wave may be considered as some superposition of various plane waves with different incidence angles. Therefore, in this case there occur oscillations too, but their amplitude is weaker than in the previous case. These oscillations may be seen in Figs. 2(*b*) and 2(*c*). The figures show that the focusing effect is observable for all crystal thicknesses, but the height and width of peaks as well as the integral intensity vary periodically with a period that is approximately equal to the extinction length. The values of the extinction length are Λ = 15.1, 24.1 and 52.7 µm for photon energies E = 8, 12 and 25 keV, respectively.

The FWHM of the focused beam depends weakly on energy and is approximately equal to 10 µm from the simulations. Our results demonstrate that in the case of hard radiation it may be possible to choose a crystal thickness when the focusing effect is well pronounced despite interference oscillations. Hence the effect may be explored for measuring the radiation energy spectrum in finite limits. We note once again that in the case of one crystal the source-to-crystal distance has to be sufficiently long.

4. Diffraction focusing of an X-ray spherical wave by two single crystals

Another kind of diffraction focusing was discovered in the case of weak absorption using two single crystals of equal thicknesses $t_1 = t_2 = t$ and a short (even zero) distance between the source and detector (Indenbom *et al.*, 1974*a*,*b*). Nevertheless, a small distance between the crystals is required to separate the transmitted and reflected beams in space. This was assumed in simulations. The secondary source was created by the same CRL as described in the preceding section. In the work of Indenbom & Suvorov (1976) this effect was used in an experiment as a kind of X-ray energy spectrometer. Effective working of the spectrometer was possible only if the source-to-detector distance was sufficiently large.

It is interesting to investigate how the beam transverse size depends on the source-to-detector distance when both crystals are of the same thickness. Fig. 4 for the first time demonstrates the results of such calculations. In the case of a Si crystal, (220) reflection and zero distance, we calculate the transverse size of the focused beam (FWHM) as Δx = 1.41 µm for E = 25 keV and t = 358 µm, Δx = 1.85 µm for E = 25 keV and t = 338 µm, and Δx = 2.01 µm for E = 12 keV and t = 324 µm. These values are less than the focused beam size in the case of one single crystal described above.

For weaker reflections the beam size increases because the focusing angular range decreases. For example, for E = 25 keV we get the mean value of Δx = 4.2 µm for Si (331) and 7.3 µm for Si (531). The mean values were obtained for the interval of t from 100 to 1000 µm. However, zero distance is not applicable for a spectrometer. Fig. 4 shows how the beam width (FWHM) increases with increasing source-to-detector distance z_1. One may see that the beam width becomes 8 µm for hard X-rays and 14 µm for soft X-rays even for a relatively small distance 100 cm. We note that this beam is not focused because the focusing condition is not met.

Hence, we may conclude that the fine effect of diffraction focusing by two single crystals is not effective for a spectrometer as was pointed out by Indenbom & Suvorov (1976). On the other hand, the focusing condition for one single crystal

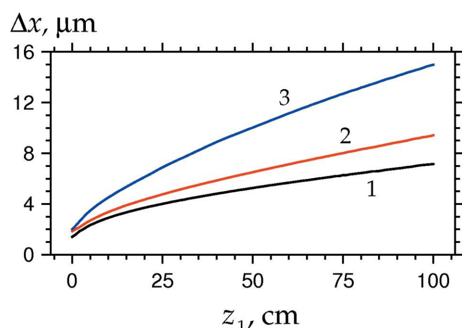

Figure 4
Variation of the twice-reflected beam width (FWHM) Δx in the case of two crystals with a source-to-detector distance z_1 for Si (220). The black curve (1) is for E = 25 keV, t = 358 µm. The red curve (2) is for E = 25 keV, t = 338 µm. The blue curve (3) is for E = 12 keV, t = 324 µm.

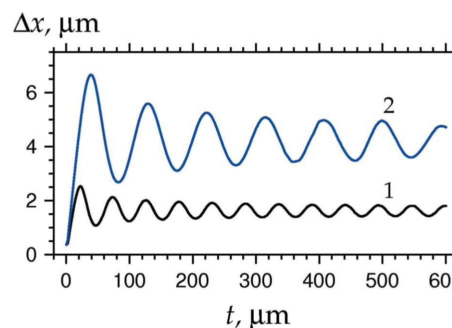

Figure 5
Variation of the twice-reflected beam width (FWHM) Δx in the case of two crystals with a crystal thickness t for zero source-to-detector distance, E = 25 keV. The black curve (1) is for Si (220), the blue curve (2) is for Si (331).

electronic reprint

demands a large source-to-detector distance that is needed simultaneously for a spectrometer (Kohn *et al.*, 2018*a*,*b*).

It is of interest that zero distance may be easily realized and investigated by means of a CRL. In order to do this, one has to focus the beam by a CRL placed at the detector and to put a system of two single crystals in-between the CRL and the detector. We have investigated this experimental setup by means of computer simulations. Fig. 5 shows the dependence of the focused beam transverse size (FWHM) on the crystal thickness *t* for two cases Si (220) and Si (331).

It follows from calculations that beam size oscillates with increasing distance. The integral intensity oscillates as well. The origin of these oscillations is the same as discussed in the preceding section. In the case of weak absorption the plane wave changes its direction periodically between the transmitted beam and the reflected one due to the extinction effect. The reflected spherical wave oscillates with approximately the same period but the amplitude of oscillations is less than for the plane wave. The focused beam width is smaller the stronger the reflection.

5. Conclusion

Computer simulations of X-ray spherical wave dynamical diffraction in one and two single crystals in the Laue case were performed with the aim of exploring the divergent beam diffraction focusing effect in an X-ray energy spectrometer as proposed in the work of Kohn *et al.* (2013). The spectrometer may be used for XFEL single-pulse monitoring. The key idea is to use an X-ray compound refractive lens for creating a divergent radiation secondary source.

We have found that the reflected beam diffraction focusing effect in the case of one single crystal may be used in both cases of strong absorption and medium or even weak absorption because the focusing effect occurs for a large source-to-detector distance. On the other hand, the diffraction focusing effect in the case of two single crystals in the twice-reflected beam is not effective because it is well pronounced only for a small source-to-detector distance. The beam transverse size increases with increasing distance.

Nevertheless, a CRL allows one to investigate the diffraction focusing effect in the case of two single crystals in the twice-reflected beam even with zero source-to-detector distance, if the detector is placed at the focus of the CRL. We have found that, in the case of weak absorption, the integral intensity as well as the focused beam transverse size oscillate with increasing crystal thickness due to the extinction effect.

References

Afanas'ev, A. M. & Kohn, V. G. (1971). *Acta Cryst.* A**27**, 421–430.

Afanasev, A. M. & Kon, V. G. (1977*a*). *Fiz. Tverd. Tela (Leningrad)*, **19**, 1775–1783.

Afanasev, A. M. & Kon, V. G. (1977*b*). *Sov. Phys. Solid State*, **19**, 1035–1040.

Aristov, V. V., Kohn, V. G., Polovinkina, V. I. & Snigirev, A. A. (1982). *Phys. Status Solidi A*, **72**, 483–491.

Aristov, V. V., Kohn, V. G. & Snigirev, A. A. (1986*a*). *Kristallographia (Moscow)*, **31**, 1059–1065.

Aristov, V. V., Kohn, V. G. & Snigirev, A. A. (1986*b*). *Sov. Phys. Crystallogr.* **31**, 626–630.

Aristov, V. V., Polovinkina, V. I., Afanas'ev, A. M. & Kohn, V. G. (1980). *Acta Cryst.* A**36**, 1002–1013.

Aristov, V. V., Polovinkina, V. I., Shmyt'ko, I. M. & Shulakov, E. V. (1978). *Pis'ma v ZhETF (Moscow)*, **28**, 6.

Aristov, V. V., Snigirev, A. A., Afanas'ev, A. M., Kohn, V. G. & Polovinkina, V. I. (1986). *Acta Cryst.* A**42**, 426–435.

Authier, A. (2005). *Dynamical Theory of X-ray Diffraction*, 3rd ed. Oxford University Press.

Indenbom, V. L., Slobodetskii, I. Sh. & Truni, K. G. (1974*a*). *ZhETF (Moscow)*, **66**, 1110–1120.

Indenbom, V. L., Slobodetskii, I. Sh. & Truni, K. G. (1974*b*). *Sov. Phys. JETP*, **39**, 542–546.

Indenbom, V. L. & Suvorov, E. V. (1976). *Pis'ma v ZhETF (Moscow)*, **23**, 485–489.

Kato, N. (1961). *Acta Cryst.* **14**, 526–532.

Kato, N. & Lang, A. R. (1959). *Acta Cryst.* **12**, 787–794.

Kohn, V. G. (1979). *Kristallographia (Moscow)*, **24**, 712–719.

Kohn, V. G. (2002). *Phys. Status Solidi B*, **231**, 132–148.

Kohn, V. G. (2017). http://kohnvict.ucoz.ru/acl/acl.htm.

Kohn, V. G., Gorobtsov, O. Y. & Vartanyants, I. A. (2013). *J. Synchrotron Rad.* **20**, 258–265.

Kohn, V. G., Smirnova, I. A., Snigireva, I. I. & Snigirev, A. A. (2018*a*). *Kristallographia (Moscow)*, **63**, 530–536.

Kohn, V. G., Smirnova, I. A., Snigireva, I. I. & Snigirev, A. A. (2018*b*). *Crystallogr. Rep.* **63**, 536–542.

Kohn, V. G., Snigireva, I. & Snigirev, A. (2000). *Phys. Status Solidi B*, **222**, 407–423.

Koz'mik, V. D. & Mihailiuk, I. P. (1978). *Pis'ma v ZhETF (Moscow)*, **28**, 673.

Lengeler, B., Schroer, C., Tümmler, J., Benner, B., Richwin, M., Snigirev, A., Snigireva, I. & Drakopoulos, M. (1999). *J. Synchrotron Rad.* **6**, 1153–1167.

Pendry, J. B. (2000). *Phys. Rev. Lett.* **85**, 3966–3969.

Pinsker, Z. G. (1978). *Dynamical Scattering of X-rays in Crystals*. Berlin, Heidelberg: Springer-Verlag.

Shulakov, E. V. & Smirnova, I. A. (2001). *Poverkhnost'. Rent. Synchr. Neutr. Study (Moscow)*, **1**, 76.

Snigirev, A., Kohn, V., Snigireva, I. & Lengeler, B. (1996). *Nature*, **384**, 49–51.

Snigirev, A., Snigireva, I., Grigoriev, M., Yunkin, V., Di Michiel, M., Vaughan, G., Kohn, V. & Kuznetsov, S. (2009). *J. Phys. Conf. Ser.* **186**, 012072.

Suvorov, E. V. & Polovinkina, V. I. (1974). *Pis'ma v ZhETF (Moscow)*, **20**, 326–329.

Takagi, S. (1962). *Acta Cryst.* **15**, 1311–1312.

electronic reprint